JCTC Journal of Chemical Theory and Computation

2-Phenylpyridine: To Twist or Not To Twist?

Kerwin D. Dobbs*,† and Karl Sohlberg‡

DuPont Central Research & Development, Experimental Station, P.O. Box 80320, Wilmington, Delaware 19880-0320, and Department of Chemistry, Drexel University, 3141 Chestnut Street, Philadelphia, Pennsylvania 19104

Received July 26, 2006

Abstract: Density functional theory methods were used to investigate the structures associated with 2-phenylpyridine, **ppy**, and several of its electronic states. The structure of **ppy** has the aromatic rings twisted with respect to one another by ∼21°, which is about half the value found for biphenyl. In comparison with **ppy**, both the isoelectronic cation, **ppyH**$^+$, and anion, **ppy**$^-$, have larger twist angles. The extent of twisting is governed by the delicate balance between π conjugation and repulsive orbital/steric interactions, and the magnitudes of these interactions were investigated by examining the torsional energy barriers for all three molecular species. In contrast, every one of the investigated open-shell structures—**ppy**$^{\bullet+}$, **ppy**$^{\bullet-}$, **ppy***, **ppyH**$^+$*****, and **ppy**$^-$*****—has coplanar aromatic rings, that is, no twist angle. Frontier molecular orbital analyses reveal that the π-type bonding between the bridging carbons becomes dominant over any repulsive orbital and steric interactions, thereby leading to coplanar rings. Also, the energetics associated with **ppy** and its various electronic states were investigated and reported.

Introduction

Materials with conjugated organic moieties, whether they be molecular, oligomeric, or polymeric in nature, are being used in devices as semiconductors or light-emitting diodes and have captured the imaginations of researchers investigating the associated structural, electronic, and optical properties.[1−3] These conjugated moieties are usually olefins (e.g., ethylene and acetylene), freely rotating aromatic rings (e.g., benzene and thiophene), rigidly linked biphenyl-like units (fluorene and carbazole), or fused aromatic rings (e.g., tetracene and pentacene). In conjunction with experimental work, the past decade has seen the fundamental properties of these conjugated materials being ascertained through quantum mechanical modeling of the actual molecular system or the repeat unit of an oligomer/polymer system.[4] By using first-principles computational chemistry methods such as density functional theory (DFT), one will obtain computational results which are accurate and reliable, thereby extending limited experimental data and allowing the confident study of systems which may be difficult to do experimentally. One such conjugated molecular system with a paucity of experimental molecular property data is 2-phenylpyridine, **ppy**.

The only existing structural information for **ppy** is obtained indirectly through the X-ray crystal structures of organometallic complexes containing **ppy** as the formally anionic ligand, **ppy**$^-$. This ligand and its derivatives are commonly found in organometallic species which are electroluminescent.[5,6] In all of these structures, the **ppy**$^-$ ligand was shown

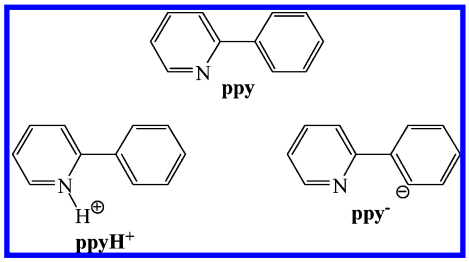

to have coplanar, or very nearly coplanar, aromatic rings. Previous computations on the neutral **ppy** molecule, however, have found the aromatic rings to be twisted with respect to

* Corresponding author e-mail: Kerwin.D.Dobbs@usa.dupont.com.
† DuPont Central Research & Development (this paper is DuPont contribution #8747).
‡ Drexel University.

10.1021/ct600242m CCC: $33.50
Published on Web 10/14/2006

each other in the range of 21−32°.[7,8] In acidic aqueous media, **ppy** is in its protonated form, **ppyH**$^+$, and may exhibit either fluorescent or phosphorescent characteristics.[9−11] Also, this experimental work resulted in qualitative arguments which suggest a twisted structure for the ground state of **ppyH**$^+$ but a planar structure for the first excited triplet state. To date, no first-principles computational chemistry data exist either for the singlet states of **ppyH**$^+$ and **ppy**$^-$ or for the first excited triplet states of all three molecular species—**ppy***, **ppyH**$^+$*, and **ppy**$^-$*.

The ionizing (electron removal/addition) of conjugated polymer chains can have profound effects on their conductivity. Oxidation/reduction creates a localized charge defect in the polymer chain known as a positive/negative polaron.[12] The radical cation, **ppy**$^{\bullet+}$, and radical anion, **ppy**$^{\bullet-}$, may be considered as models for single-charged defects in polymers which contain **ppy** as a comonomer. What is unknown is the effect on the molecular structure of **ppy** upon ionization.

Computational Model

DFT methods are used to understand the structure and energetics of **ppy** and its various electronic states. The first task is to firmly establish the equilibrium structure of **ppy** and the energy maxima (at $\phi = 0°$ and 90°) for rotation about the CC bond linking the two aromatic rings.

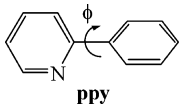

ppy

A full torsional energy profile is not necessary because it has been investigated previously.[8]

The second task is to investigate the structural and energetic properties of the isoelectronic cationic and anionic states of **ppy**. For the protonation of **ppy** to form **ppyH**$^+$, a proton is attached to the pyridine nitrogen

$$\mathbf{ppy} + \mathrm{H}^+ \rightarrow \mathbf{ppyH}^+ \ldots \Delta H$$

The release of energy is known as the proton affinity of **ppy** and is defined as the negative enthalpy, $-\Delta H$, for the above reaction. The isoelectronic anion, **ppy**$^-$, of interest is the one in which H$^+$ is removed from the phenyl carbon "ortho" to the CC bridge between the two rings of **ppy**, and the enthalpy for this reaction

$$\mathbf{ppy} \rightarrow \mathbf{ppy}^- + \mathrm{H}^+ \ldots \Delta H$$

is known as the deprotonation energy of **ppy**. In addition, the torsional barriers of **ppyH**$^+$ and **ppy**$^-$ at ϕ values of 0° and 90° are computed and compared with the **ppy** results.

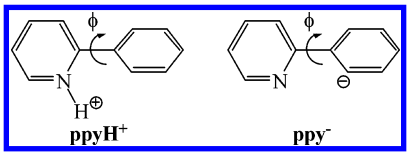

Third, an electron is subtracted and added to **ppy** to form, respectively, the radical cation, **ppy**$^{\bullet+}$, and the radical anion, **ppy**$^{\bullet-}$, and the computed structures of these two charged, radical species are compared to that of **ppy**. In addition, the ionization potential (IP) and electron affinity (EA) of **ppy** to form **ppy**$^{\bullet+}$ and **ppy**$^{\bullet-}$, respectively,

$$\mathrm{IP} = E(\mathbf{ppy}^{\bullet+}) - E(\mathbf{ppy})$$

may be determined as "adiabatic" or "vertical" values. The

$$\mathrm{EA} = -[E(\mathbf{ppy}^{\bullet-}) - E(\mathbf{ppy})]$$

adiabatic value is the energy difference between the charged, radical species in its relaxed (optimized) geometry and the respective neutral, singlet species in its relaxed geometry. For the vertical value, the energy difference is between the charged, radical species at the geometry of its neutral state and the neutral species in its relaxed geometry. Both the adiabatic and vertical IPs and EAs are computed in order to determine the effects of structure on these energy values.

As part of the third task, the focus on open-shell analogues continues with the comparison of the first excited triplet states, **ppy***, **ppyH**$^+$*, and **ppy**$^-$*, with respect to their singlet ground states, **ppy**, **ppyH**$^+$, and **ppy**$^-$. In addition to examining the structural differences between the singlet and triplet molecular species, the singlet−triplet energy differences are also investigated. The adiabatic energy difference, $\Delta E_{ad}(S_0 \rightarrow T_1)$, is the energy needed to excite a molecule from its singlet ground-state geometry to the relaxed geometry of its first excited triplet state. An alternative method to use is time-dependent DFT (TDDFT),[13−16] which has proven to be most successful for low-energy excitations.[17,18]

Table 1. Inter-Ring Distances (CC in Angstroms) and Twist Angles (ϕ in Degrees) for **ppy**[a]

	CC		ϕ	
basis sets	BP86	B3LYP	BP86	B3LYP
6-31G(d)	1.492	1.488	15.0 (16.0)	18.2 (19.3)
6-311G(d)	1.490	1.488	18.1 (19.4)	20.4 (21.8)
6-311G(2d,2p)	1.489	1.486	18.2 (19.4)	20.8 (21.9)

[a] The numbers in parentheses are the alternate dihedral angles between the aromatic rings (see text).

Computational Details

All calculations were performed with the Gaussian 03 suite of programs.[19] The neutral, singlet **ppy** structure was optimized by DFT with the density functionals BP86[20,21] and B3LYP[22,23] in conjunction with a few selected basis sets: 6-31G(d),[24] 6-311G(d),[25] and 6-311G(2d,2p).[26] The hybrid functional B3LYP has proven to be good for the rotational barriers of biphenyl[27] as well as for relative energetics in general. The pure BP86 functional was chosen mainly because of the enhanced performance gains of the calculations using this functional compared to B3LYP. Pure functionals are able to take advantage of using density fitting basis sets which expand the density in a set of atom-centered functions when computing the Coulomb interaction instead of computing all of the two-electron integrals.[28,29] Table 1 presents selected metric parameters for the equilibrium structure of **ppy** at several different levels of theory. For the purposes of this study, the metric parameters of interest

Table 2. Inter-Ring Distances (CC in Angstroms) and Torsional Barrier Heights (kcal/mol) for **ppy** at Twist Angle $\phi = 0.0°$ and 90.0° for Different Levels of Computation

		BP86			B3LYP		
ϕ	basis sets	CC	ΔH	ΔG	CC	ΔH	ΔG
0.0	6-31G(d)	1.493	0	1	1.491	0	1
	6-311G(d)	1.492	0	1	1.490	0	1
	6-311G(2d,2p)	1.491	0	1	1.489	0	1
90.0	6-31G(d)	1.504	4	6	1.498	4	5
	6-311G(d)	1.501	4	5	1.497	4	5
	6-311G(2d,2p)	1.500	4	5	1.496	4	5

are the inter-ring CC distance and the twist angle, ϕ, which is the dihedral angle defined as N1−C2−C2′−C1′:

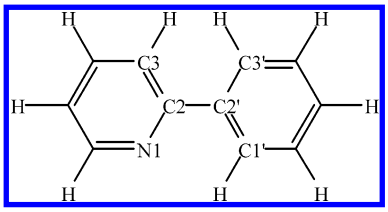

Values for the dihedral angle C3−C2−C2′−C3′ are also given in Table 1 in parentheses and turn out to be noticeably different from the defined twist angle because of the nonplanarity of the two aromatic rings.[8] Because each optimized geometry was characterized by a harmonic vibrational frequency analysis at the same level of computation, the calculated frequencies were used to determine zero-point energy and vibrational thermal corrections (at 298.15 K) for use in determining energetic properties unless otherwise stated. To determine rotational barriers of **ppy**, two structures of **ppy** were fully optimized with the twist angle, ϕ, being constrained to 0° and 90°. The enthalpic and free energy torsional barrier heights as well as the inter-ring CC distances for **ppy** at $\phi = 0°$ and 90° are presented in Table 2.

The remaining calculations were all done with the B3LYP functional, and any energetic properties which involved **ppy** utilized the B3LYP/6-311G(2d,2p) geometry of **ppy**. To investigate the structures of the isoelectronic cationic (**ppyH**$^+$) and anionic (**ppy**$^-$) singlet states of **ppy**, the polarized triple-ζ basis sets, 6-311G(2d,2p), and the diffuse basis sets, 6-311+G(2d,2p) and 6-311++G(2d,2p),[30] were used. Two energy minima exist for **ppy**$^-$: a local minimum at $\phi < 50°$ and a global minimum at $\phi = 180°$. For this study, the former structure is of greater interest because this rotational isomer closely resembles the **ppy** anionic ligand in organometallic structures. The inter-ring CC distances and twist angles at the different levels of computation are presented in Table 3. A computational procedure, similar to the one employed for the neutral **ppy** species, was used to determine the inter-ring CC bond lengths and the torsional barrier heights (at $\phi = 0°$ and 90°) of **ppyH**$^+$ and **ppy**$^-$ but only at the B3LYP/6-311+G(2d,2p) level (see Table 4). As can be seen in Table 3, the extra set of diffuse functions (for H) does not alter the structures of these ionic species. The proton affinity and deprotonation energy of **ppy** were computed at the B3LYP/6-311++G(2d,2p) level and are presented in Table 5 as the energy property $\Delta H(H^+)$.

Table 3. Inter-Ring Distances (CC in Angstroms) and Twist Angles (ϕ in Degrees) for **ppyH**$^+$ and **ppy**$^-$, Using the B3LYP Hybrid Functional and the Indicated Basis Sets

	ppyH$^+$		**ppy**$^-$	
basis sets	CC	ϕ	CC	ϕ
6-311G(2d,2p)	1.463	33.0 (33.6)	1.488	43.1 (41.8)
6-311+G(2d,2p)	1.464	33.1 (33.7)	1.489	48.1 (46.4)
6-311++G(2d,2p)	1.464	33.1 (33.7)	1.489	48.2 (46.4)

Table 4. Inter-Ring Distances (CC in Angstroms) and Torsional Barrier Heights (kcal/mol) for **ppyH**$^+$ and **ppy**$^-$ at Twist Angle $\phi = 0.0°$ and 90.0° for the B3LYP/6-311+G(2d,2p) Level of Theory

	ppyH$^+$			**ppy**$^-$		
ϕ	CC	ΔH	ΔG	CC	ΔH	ΔG
0.0	1.467	1	2	1.497	2	3
90.0	1.483	3	4	1.500	0	1

Table 5. Energy Properties for **ppyH**$^+$ and **ppy**$^-$ at the B3LYP/6-311++G(2d,2p) Level of Theory[a]

property	**ppyH**$^+$	**ppy**$^-$
$\Delta H(H^+)$	10 (230)	17 (398)
$\Delta E_{ad}(S_0 \rightarrow T_1)$	2.6 (60)	0.8 (19)
$\Delta E_{TDDFT}(S_0 \rightarrow T_1)$	2.9 (67)	1.4 (32)

[a] Energies are given in eV with numbers in parentheses given in kcal/mol.

Table 6. Inter-Ring Distances (CC in Angstroms) for **ppy**, **ppy**$^{\bullet+}$, **ppy**$^{\bullet-}$, **ppy***, **ppyH**$^+$*, and **ppy**$^-$* Using the B3LYP Hybrid Functional

basis sets	**ppy**	**ppy**$^{\bullet+}$	**ppy**$^{\bullet-}$	**ppy***	**ppyH**$^+$*	**ppy**$^-$*
6-311G(2d,2p)	1.486	1.443	1.434	1.387	1.398[a]	1.425
6-311+G(2d,2p)		1.444	1.435		1.399	1.426
6-311++G(2d,2p)		1.444	1.435		1.399	1.426

[a] The aromatic rings are coplanar at all levels of theory for all open-shell molecules with the exception of this one, in which the optimized twist angle is actually 1.1° at this particular level of theory.

For the neutral, triplet state **ppy***, the structure and frequencies were computed using the 6-311G(2d,2p) basis sets. These same basis sets plus the two diffuse versions were used to compute the structures and frequencies of the remaining open-shell molecules: the ionic radical doublets, **ppy**$^{\bullet+}$ and **ppy**$^{\bullet-}$, as well as the ionic triplets, **ppyH**$^+$* and **ppy**$^-$*. Because the two aromatic rings in each of these optimized structures are coplanar, only the inter-ring CC bond lengths are presented in Table 6.

The energetic properties of the neutral, singlet state of **ppy** with respect to the three open-shell species, **ppy***, **ppy**$^{\bullet+}$, and **ppy**$^{\bullet-}$, were obtained at the B3LYP/6-311++G(2d,2p) level of computation and are presented in Table 7. Each of the adiabatic IP, EA, and $\Delta E_{ad}(S_0 \rightarrow T_1)$ values are determined from the energy difference between the **ppy** structure and each of the three structure-optimized open-shell states. To determine the vertical IP and EA values, single-point energy calculations were first carried out at the designated computational level for each of the open-shell

Table 7. Energy Properties for **ppy** Computed at the B3LYP/6-311++G(2d,2p) Level of Theory[a]

property	energy
IP_{ad}	8.0 (185)
IP_{vert}	8.2 (189)
EA_{ad}	0.3 (6)
EA_{vert}	−0.1 (−2)
$\Delta E_{ad}(S_0 \rightarrow T_1)$	2.8 (65)
$\Delta E_{TDDFT}(S_0 \rightarrow T_1)$	3.2 (73)

[a] Energies are given in eV with numbers in parentheses given in kcal/mol.

species at the singlet **ppy** geometry. Then, the vertical energy is determined by subtracting the energy of the singlet **ppy** from each of these new single-point energies [e.g., $IP_{vert} = E(\mathbf{ppy}^{\bullet+}@\mathbf{ppy}\ \text{geom.}) - E(\mathbf{ppy})$]. By their nature, vertical energies do not have corrections for zero-point energy and vibrational thermal effects. To complete the energetic picture for the triplet energy surface relative to the singlet one, TDDFT computations were carried out for the first seven excited triplet states on the singlet structure of **ppy**. Only the excitation energy to the first excited triplet state, $\Delta E_{TDDFT}(S_0 \rightarrow T_1)$, is presented in Table 7. In a manner similar to the one just described for **ppy**, the energetics for $\mathbf{ppyH}^+$ and $\mathbf{ppy}^-$ relative to their respective triplet states have been completed and are reported as $\Delta E_{ad}(S_0 \rightarrow T_1)$ and $\Delta E_{TDDFT}(S_0 \rightarrow T_1)$ values in Table 5.

Results and Discussion

ppy. The equilibrium gas-phase structure of **ppy** is known only through computational results, and the highest-level calculations to date may be found in two recent reports in the literature. In a thermochemical study of phenylpyridine isomers, da Silva et al.[7] obtained an inter-ring CC distance of 1.488 Å and a twist angle of 20.7° at the B3LYP/6-31G(d) level of theory. In examining the torsional barrier of **ppy**, Göller and Grummt[8] used four different methods: HF/6-31G(d), MP2/6-31G(d), BPW91/6-31+G(d), and B3LYP/6-31+G(d). Respectively, these methods yielded inter-ring CC bond lengths of 1.491, 1.479, 1.491, and 1.489 Å as well as twist angles of 27.9°, 31.5°, 26.7°, and 21.9°. We wanted to see if the inter-ring CC distance and the twist angle of **ppy** would greatly change either as the basis set became larger or in switching from a pure density functional (BP86) to a hybrid one (B3LYP). An exhaustive study with a variety of basis sets and density functionals was unnecessary because experimental structure information is not available for judging the accuracy of the computed methods. As indicated in Table 1, our best DFT values, (BP86;B3LYP)/6-311G(2d,2p), for these metric parameters essentially agree with previous computational studies in that the CC bond length is about 1.49 Å and the twist angle is uncertain (ours is 18−21°). This latter uncertainty is probably due to the shallowness of the torsional potential energy surface where the aromatic rings are nearly coplanar (vide infra and ref 8). The MP2 results of Göller and Grummt indicate a CC bond length which is shorter by 0.01 Å compared to all of the DFT results. A similar result was found in a definitive computational study of biphenyl by Arulmozhiraja and Fujii.[27] Also, the highest-level DFT computations in this latter study yielded a twist angle of ∼40° for biphenyl. The second dihedral angle between the aromatic rings (numbers in parentheses in Table 1) is about 1° larger than the defined twist angle and is indicative of nonplanar rings. In fact, all of the computational methods in the current study agree that the largest distortion from planarity in each ring is at the bridging carbon atom.

Just as in the isoelectronic biphenyl molecule, the twist angle between the two aromatic rings is a delicate balance between electronic and steric effects. The two major electronic effects are the degree of π conjugation between the two rings, leading to coplanar rings, and the repulsive orbital interactions between the π systems of each ring, leading to a twisted structure. Repulsive steric interactions between the ortho hydrogens on different rings tend to direct the rings to be perpendicular to one another.

One way to gauge the magnitude of these effects is to compute the torsional barriers of **ppy** at $\phi = 0°$ (rings are coplanar) and at $\phi = 90°$ (rings are perpendicular), and the corresponding enthalpic and free energy values are presented in Table 2. Within the reliability of the methods being used, the torsional barriers turned out to be independent of the basis set and density functional. There is no enthalpic barrier for making the rings coplanar, and the corresponding free energy barrier is only 1 kcal/mol. Concurrently, the CC bond length has lengthened by no more than 0.003 Å. Coplanarity would maximize the repulsive interactions between the two rings, but these interactions must already be well-balanced by π conjugation because of the small rotational barrier and minor effect on the inter-ring CC distance. This small energy barrier for coplanarity not only explains the wide range in optimized twist angles from different computational methods but also would predict difficulty in obtaining a small uncertainty for the twist angle in an experimental structure.

On the other hand, the enthalpic (4 kcal/mol) and free energy (5 kcal/mol) barriers for making the rings perpendicular are more substantial. Also, there is a noticeable lengthening of the inter-ring CC distance by about 0.01 Å toward a typical CC single bond length. Maximizing the twist angle essentially eliminates any repulsive orbital and steric interactions between the aromatic rings, but it also disrupts any π-type bonding between the two rings. Göller and Grummt[8] had obtained similar magnitudes for the torsional barriers of **ppy**, but they had claimed that a three-center−four-electron interaction between the nitrogen and ortho C−H bond on the neighboring ring (N1···H1′C1′) contributed to the very low barrier for $\phi = 0°$. We cannot support such a claim, which was based solely on geometrical arguments. Overall, our computed results point to weaker repulsive orbital and steric interactions compared to the π-electron delocalization between the rings. The BP86 functional has proven itself to provide structural and torsional energy results comparable to those with B3LYP. For the rest of this investigation, however, the B3LYP functional was used, mainly because of its proven success for reaction energetics.[31]

$\mathbf{ppyH}^+$ and $\mathbf{ppy}^-$. To date, there have been no computational chemistry reports in the literature for either the protonated or anionic forms of **ppy** in order to determine

if they have twist angles and, if so, the energy barriers for coplanar as well as perpendicular rings. We have high confidence in the structure results for **ppy** with the 6-311G(2d,2p) basis sets. To gauge basis set convergence for the ionic forms of **ppy**, however, diffuse functions were initially added to the heavy atoms of this basis set [6-311+G(2d,2p)], and then to the hydrogens [6-311++G(2d,2p)], and selected optimized metric parameters with the B3LYP functional are presented in Table 3. With the first set of diffuse functions, the inter-ring CC bond length in either ionic molecule increases by only 0.001 Å while the twist angle for **ppyH**$^+$ increases by only 0.1°. But, the **ppy**$^-$ twist angle is more sensitive to the addition of the first set of diffuse functions, increasing by 5°. No significant changes in metric parameters occur with the addition of diffuse functions for hydrogens. Just like for **ppy**, the rings are nonplanar for either ionic species. This distortion in planarity (see numbers in parentheses in Table 3) is smaller for **ppyH**$^+$ than for **ppy**, but it is larger for **ppy**$^-$. In fact, the second dihedral angle is actually *smaller* than the defined twist angle by nearly 2°, which may be indicative of a repulsive steric interaction between the ortho hydrogens being less than the repulsive interaction between the lone pairs on the nitrogen and the anionic carbon atom.

Compared to **ppy** at the same level of theory, B3LYP/6-311G(2d,2p), the inter-ring CC bond length is 0.023 Å shorter and the twist angle is about 12° larger for **ppyH**$^+$. The shorter bond length points to a weaker orbital repulsion compared to the π conjugation, while the larger twist angle is the result of two sets of ortho-hydrogen steric interactions. For **ppy**$^-$, the inter-ring CC bond length is slightly longer by 0.002 Å, while the twist angle is noticeably larger by 22° compared to that for **ppy**. Because **ppy** and **ppy**$^-$ both have the same number of ortho-hydrogen steric interactions, the much larger twist angle in **ppy**$^-$ must be the result of orbital repulsions, most likely, the repulsive interaction between the lone pairs on the nitrogen and the anionic carbon atom.

The torsional energy barriers and inter-ring CC distances of **ppyH**$^+$ and **ppy**$^-$ at the B3LYP/6-311+G(2d,2p) level are presented in Table 4. When compared to **ppy**, the resistance to ring coplanarity for these ions is somewhat greater. Just like for **ppy**, the ortho-hydrogen steric interactions are at a maximum for coplanar rings in **ppyH**$^+$, but two sets of these steric interactions (compared to only one set in **ppy**) have yielded a slightly larger barrier (by 1 kcal/mol) and a slightly longer (by 0.003 Å) CC bond compared to the relaxed structure of **ppyH**$^+$. For **ppy**$^-$, the repulsive lone-pair interaction and π overlap are both maximized for coplanar rings, but the apparently stronger repulsive interaction results in a rotational barrier 2 kcal/mol larger than that in **ppy**, while the CC bond has lengthened by 0.008 Å compared to that in the relaxed structure of **ppy**$^-$. The rotational barrier at 90° for **ppyH**$^+$ is similar to that of **ppy**, and the CC bond is 0.019 Å longer. These results are a reflection of disrupting the π conjugation (again, the stronger interaction) and eliminating any steric repulsions between the rings. In contrast, making the rings perpendicular for **ppy**$^-$ has no enthalpic barrier, a free energy barrier of 1 kcal/mol, and a longer (by 0.011 Å) CC bond between the rings. Although the π conjugation has been disrupted, it has been almost equally balanced by the easing of the repulsive interaction between the lone pairs on the nitrogen and the anionic carbon atom.

ppy$^{\bullet+}$, ppy$^{\bullet-}$, ppy*, ppyH$^+$*, and ppy$^-$*. To our knowledge, neither the two radical ions nor the three triplet species have been studied computationally. Using the B3LYP hybrid functional, the optimized geometries for these open-shell molecules were determined with the 6-311G(2d,2p) basis sets, and the effects to the inter-ring CC bond lengths of adding diffuse functions to the heavy atoms, and then to hydrogen, for the charged species is presented in Table 6. As was found for **ppyH**$^+$ and **ppy**$^-$, the inter-ring distances for all of the ionic molecules increase by 0.001 Å with the addition of diffuse functions for carbon and nitrogen, but no further change in this metric parameter occurs when also adding diffuse functions for hydrogen.

The structures of all of these open-shell species are rather interesting because each of the inter-ring CC bond lengths is much shorter than that computed for the corresponding closed-shell species and the aromatic rings in each structure are coplanar. As a point of reference, DFT computations for the isoelectronic biphenyl open-shell molecules[27,32] have yielded similar conclusions with the exception that the biphenyl radical cation has a twist angle[27] which is in agreement with experimental resonance Raman spectra.[33] Compared to **ppy**, the B3LYP/6-311G(2d,2p) values for the inter-ring bond lengths of **ppy**$^{\bullet+}$ and **ppy**$^{\bullet-}$ are shorter by 0.043 and 0.052 Å, respectively, whereas this bond length is still even shorter, by 0.099 Å, for **ppy***. When compared to the closed-shell molecules **ppyH**$^+$ and **ppy**$^-$, the shortening of the inter-ring CC bond for the corresponding open-shell molecules, **ppyH**$^+$***** and **ppy**$^-$*****, is similar (0.065 and 0.063 Å, respectively). At first glance, the shorter inter-ring distances and coplanar aromatic rings seem to be counterintuitive. These structural preferences, however, are easily explained by examining the respective frontier molecular orbitals.

Figure 1 compares the highest occupied molecular orbitals (HOMOs) and lowest unoccupied molecular orbital (LUMOs) of **ppy**, **ppy**$^{\bullet+}$, **ppy**$^{\bullet-}$, and **ppy***.[34,35] The HOMO of **ppy** represents a π*-like repulsive interaction between the two rings, contributing to the twist angle of ~21°, whereas the corresponding LUMO displays π-like bonding between the two bridging carbon atoms. Although the HOMO and LUMO of **ppy**$^{\bullet+}$ are identical to those of **ppy**, there is now one less electron in the HOMO of **ppy**$^{\bullet+}$, which leads to orbital repulsion being reduced and π conjugation becoming dominant. The concomitant structural effects are a shorter distance between the rings and a twist angle of zero. π bonding between the bridging carbons exists for the LUMO of **ppy**. Therefore, adding an electron to this LUMO to create **ppy**$^{\bullet-}$ results in an increase in the π conjugation between the aromatic rings (see the HOMO of **ppy**$^{\bullet-}$), which overwhelms the existing repulsive π*-like interaction (see the HOMO−1 of **ppy**$^{\bullet-}$). Again, this dominant π-bonding interaction leads to a shorter inter-ring CC bond and coplanar rings when compared to the **ppy** structure. Now, what would

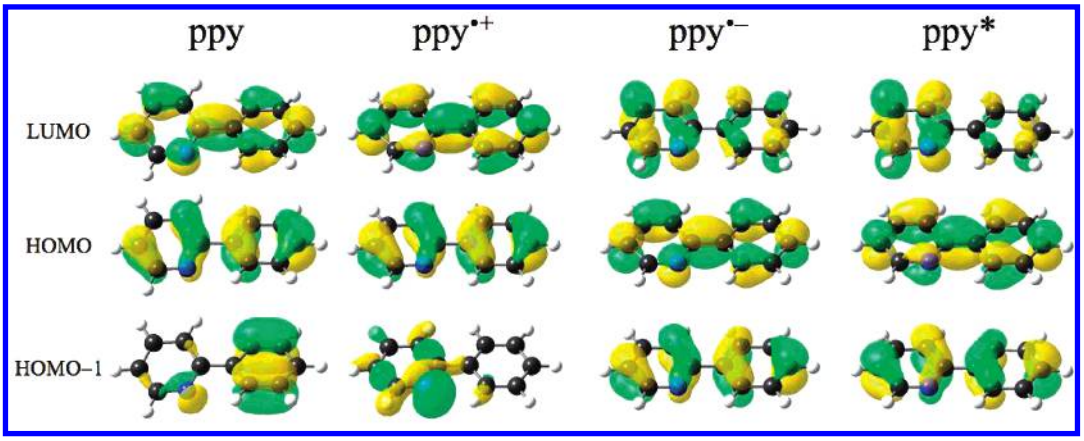

Figure 1. Frontier molecular orbitals for **ppy**, **ppy**$^{\bullet+}$, **ppy**$^{\bullet-}$, and **ppy*** which explain the shorter inter-ring CC bond distances and coplanar aromatic rings of the open-shell molecules compared to **ppy**.

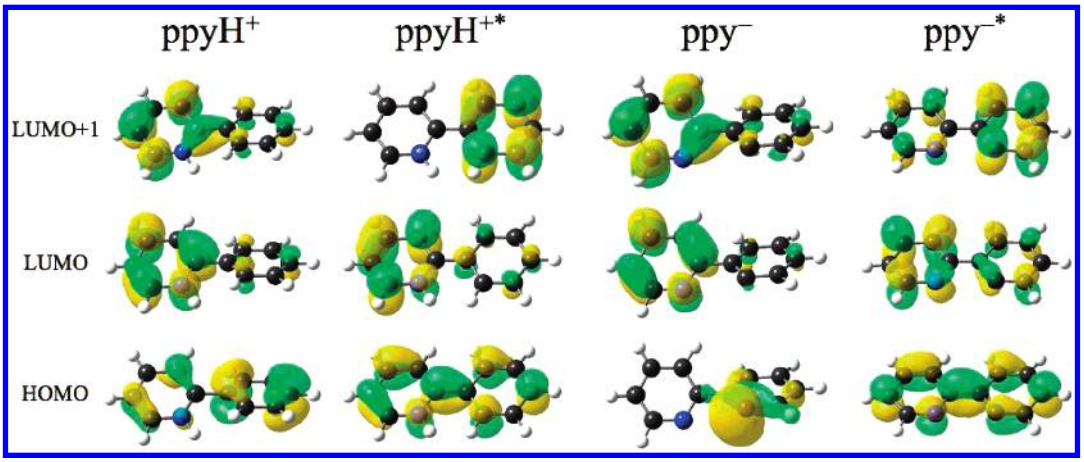

Figure 2. Frontier molecular orbitals for **ppyH**$^{+}$, **ppyH**$^{+}$***, **ppy**$^{-}$, and **ppy**$^{-}$*** which explain the shorter inter-ring CC bond distances and coplanar aromatic rings of the triplet molecules compared to their respective singlet analogues.

the result be of combining the effects seen in **ppy**$^{\bullet+}$ and in **ppy**$^{\bullet-}$, that is, to reduce the orbital repulsion, as in **ppy**$^{\bullet+}$, and increase the π conjugation, as in **ppy**$^{\bullet-}$? As it turns out, this is exactly what happens with the triplet state of **ppy**. For **ppy***, the frontier orbitals are nearly the same as those for **ppy**$^{\bullet-}$, but the electron occupancy is different. One electron is in the π-like HOMO of **ppy***, but now, there is only one electron in the π*-like HOMO$-$1. This combined effect is reflected in the much shorter CC bridge bond compared to that in **ppy**, which is essentially the sum of the bond-shortening effects found in the radical ions (0.043 Å + 0.052 Å = 0.097 Å $\approx$ 0.99 Å).

The explanation for the structural preferences found in **ppyH**$^{+}$*** and **ppy**$^{-}$*** relies on comparing the frontier orbitals of these triplet molecules with their respective singlet analogues (see Figure 2). By examining only the LUMOs of **ppyH**$^{+}$ and **ppy**$^{-}$, it is difficult to imagine how the π-bonding HOMOs came about in forming **ppyH**$^{+}$*** and **ppy**$^{-}$***. A closer look at the LUMO+1 orbitals of the singlet species, however, reveals the beginning of π overlap between the bridging carbons. The obvious π-bonding in the HOMOs of the triplet molecules is actually the result of the linear combination of the LUMO and LUMO+1 of the respective singlet species. As expected, this π bonding between the two aromatic rings explains a twist angle of zero for **ppyH**$^{+}$*** and **ppy**$^{-}$***.

Energetic Properties. The energetic properties of the singlet state of **ppy** with respect to the open-shell species, **ppy**$^{\bullet+}$, **ppy**$^{\bullet-}$, and **ppy***, were computed at the B3LYP/6-31++G(2d,2p) level and may be found in Table 7. The adiabatic ionization potential, IP_{ad}, of **ppy** to form the radical cation, **ppy**$^{\bullet+}$, is 8.2 eV and is not significantly different from the experimental ionization potential of 8.16 eV for the isoelectronic biphenyl molecule.[36] The vertical ionization potential, IP_{vert}, of **ppy** is 0.2 eV higher than the IP_{ad} value, and this difference is a measure of the structural relaxation energy for the ionization process. To form the radical anion, **ppy**$^{\bullet-}$, the computed adiabatic electron affinity, EA_{ad}, of **ppy** is 0.3 eV. As indicated by the vertical electron affinity, EA_{vert}, the structural relaxation energy for creating this anion is 0.4 eV. Several benchmark computational investigations of adiabatic ionization potentials and electron affinities have concluded that DFT methods, similar to the one in this study, have an average error in accuracy of 0.1$-$0.2 eV.[37−40]

The adiabatic energy difference, ΔE_{ad}, between the ground state of **ppy** and its corresponding triplet state is 2.8 eV. The larger value of 3.2 eV for ΔE_{TDDFT} provides an upper bound for the $S_0 \rightarrow T_1$ excitation energy and is indicative of the **ppy*** structure being very different from the corresponding singlet structure (vide supra).

The energetic properties of the two charged, isoelectronic states of **ppy**, **ppyH**$^{+}$, and **ppy**$^{-}$ at the B3LYP/6-311++G-

(2d,2p) level are presented in Table 5. Protonation of **ppy** is essentially the addition of H^+ to the nitrogen of the pyridine ring. The computed proton affinity for creating $\mathbf{ppyH}^+$ is 230 kcal/mol, which is very similar to the accepted experimental proton affinity of 222 kcal/mol for pyridine.[41] Deprotonation of **ppy** is analogous to deprotonation of benzene: H^+ is removed from the phenyl ring, leaving behind a negatively charged carbon. To form $\mathbf{ppy}^-$, the computed enthalpy of deprotonation is 398 kcal/mol, which very closely agrees with the experimental enthalpy of deprotonation of 401.7 kcal/mol for benzene.[42]

From the data in Table 5, the energetic picture of the triplet energy surface for $\mathbf{ppyH}^+$ relative to the singlet one is similar to that of **ppy** but very different from that of $\mathbf{ppy}^-$. Compared to **ppy**, the singlet−triplet energy difference, ΔE_{ad}, for $\mathbf{ppyH}^+$ is 0.2 eV lower at 2.6 eV. The upper bound for the $S_0 \rightarrow T_1$ excitation energy of $\mathbf{ppyH}^+$ is 2.9 eV and is 0.3 eV lower than the corresponding value for **ppy**. When **ppy** is in acidic media as $\mathbf{ppyH}^+$, the lowest phosphorescent peak is experimentally determined to be 2.89 eV.[10] This experimental energy value is closest to the computed ΔE_{TDDFT} value of 2.9 eV, which may indicate that the molecular structure of the excited triplet state more closely resembles that of the singlet state before losing its energy in the emission process. The ΔE_{ad} value of 0.8 eV between the singlet ground state of $\mathbf{ppy}^-$ and its first excited triplet state is about 3 times smaller than the corresponding values for **ppy** and $\mathbf{ppyH}^+$.

Conclusion

Density functional theory methods were used to investigate the structures and energetics associated with 2-phenylpyridine, **ppy**, and several of its electronic states. The structure of **ppy** has an inter-ring CC bond length of 1.49 Å, and the aromatic rings are twisted with respect to one another by ~21°, which is about half the value found for biphenyl. The extent of twisting is governed by the delicate balance between π conjugation and repulsive orbital/steric interactions, and the magnitudes of these interactions were investigated by examining the torsional energy barriers. For coplanar rings, the torsional free energy barrier is only 1 kcal/mol, indicating that any repulsive interaction between the two rings is well-balanced by π conjugation. Whereas for perpendicular rings, the torsional free energy barrier is larger at 5 kcal/mol, most likely the result of rupturing any π-type bonding between the rings. The aforementioned metric parameters and energetics were computed at the B3LYP/6-311G(2d,2p) level, whereas the metric parameters and energetics summarized in the following paragraphs were computed at the B3LYP/6-311++G(2d,2p) level.

In comparison with **ppy**, the isoelectronic cation, $\mathbf{ppyH}^+$, has a larger twist angle (33°) which is explained by the extra set of ortho-hydrogen steric interactions. These repulsive interactions, however, are weak compared to π conjugation, as evidenced by the torsional free energy barriers at twist angles of 0° and 90° being 2 and 4 kcal/mol, respectively. The isoelectronic anion, $\mathbf{ppy}^-$, has an even larger twist angle of 48°, which is primarily due to the repulsive interaction between the lone pairs on the pyridine nitrogen and on the anionic carbon of the phenyl ring. This lone-pair repulsion is significant enough to yield a torsional barrier of 3 kcal/mol for coplanar rings and to nearly counterbalance π conjugation as evidenced by a torsional barrier of 1 kcal/mol for perpendicular rings. When $\mathbf{ppy}^-$ is used as an organometallic ligand, the lone-pair repulsion is obviously of no consequence because these electrons are now involved in bonding with the metal and do not interfere with coplanarization of the rings. As expected, the proton affinity (230 kcal/mol) and deprotonation energy (398 kcal/mol) of **ppy** are very similar to the experimental values for pyridine and benzene, respectively.

Every one of the investigated open-shell structures—$\mathbf{ppy}^{\bullet+}$, $\mathbf{ppy}^{\bullet-}$, **ppy***, $\mathbf{ppyH}^+$*****, and $\mathbf{ppy}^-$*****—has no twist angle between the aromatic rings. A frontier orbital analysis which compares each open-shell molecule with its closed-shell counterpart reveals that the π-type bonding between the bridging carbons becomes dominant over any repulsive orbital and steric interactions, thereby leading to coplanar rings. The predicted ionization potential (8.2 eV), electron affinity (0.3 eV), and singlet−triplet energy difference (2.8 eV) of **ppy** are of high enough quality to present a challenge for experimental work to reproduce. The energy required to form the triplet species, $\mathbf{ppyH}^+$*****, from the ground-state singlet, $\mathbf{ppyH}^+$, is computed to be 2.6 eV, yet experimental phosphorescence studies have found the lowest triplet energy to be 2.89 eV, which is closer to the ΔE_{TDDFT} value of 2.9 eV. Because UV−vis data are sensitive to molecular structure, the good agreement between ΔE_{TDDFT} and experimental results may indicate that the molecular structure of the excited triplet state in the experiment more closely resembles that of the singlet state before losing its energy in the emission process. The very small singlet−triplet energy gap for $\mathbf{ppy}^-$ (0.8 eV) indicates an easy transformation to $\mathbf{ppy}^-$***** under applied voltage. When $\mathbf{ppy}^-$ is used as an organometallic ligand, the overall planar system of the triplet species may be connected to the electroluminescent properties of the organometallic species, but further computational work is necessary to establish a firm connection.

Supporting Information Available: Optimized coordinates and corresponding total energies for all of the molecules (26 pages). This information is available free of charge via the Internet at http://pubs.acs.org.

References

(1) Jenekhe, S. A. *Chem. Mater.* **2004**, *16*, 4381.

(2) Bendikov, M.; Wudl, F.; Perepichka, D. F. *Chem. Rev.* **2004**, *104*, 4891.

(3) Kottas, G. S.; Clarke, L. I.; Horinek, D.; Michl, J. *Chem. Rev.* **2005**, *105*, 1281.

(4) Bredas, J.-L.; Beljonne, D.; Coropceanu, V.; Cornil, J. *Chem. Rev.* **2004**, *104*, 4971.

(5) Grushin, V. V.; Herron, N.; LeCloux, D. D.; Marshall, W. J.; Petrov, V. A.; Wang, Y. *Chem. Commun.* **2001**, 1494.

(6) Brooks, J.; Babayan, Y.; Lamansky, S.; Djurovich, P. I.; Tsyba, I.; Bau, R.; Thompson, M. E. *Inorg. Chem.* **2002**, *41*, 3055.

(7) Silva, M. A. V. R. d.; Matos, M. A. R.; Rio, C. A.; Morais, V. M. F.; Wang, J.; Nichols, G.; Chickos, J. S. *J. Phys. Chem. A* **2000**, *104*, 1774.

(8) Göller, A.; Grummt, U.-W. *Chem. Phys. Lett.* **2000**, *321*, 399.

(9) Kubin, J.; Testa, A. C. *J. Photochem. Photobiol., A* **1994**, *83*, 91.

(10) Sarkar, A.; Chakravorti, S. *J. Lumin.* **1995**, *65*, 163.

(11) Pohlers, G.; Virdee, S.; Scaiano, J. C.; Sinta, R. *Chem. Mater.* **1996**, *8*, 2654.

(12) André, J.-M.; Delhalle, J.; Brédas, J.-L. *Quantum Chemistry Aided Design of Organic Polymers: An Introduction to the Quantum Chemistry of Polymers and its Applications*; World Scientific: New Jersey, 1991; Vol. 2.

(13) Runge, E.; Gross, E. K. U. *Phys. Rev. Lett.* **1984**, *52*, 997.

(14) Bauernschmitt, R.; Ahlrichs, R. *Chem. Phys. Lett.* **1996**, *256*, 454.

(15) Casida, M. E.; Jamorski, C.; Casida, K. C.; Salahub, D. R. *J. Chem. Phys.* **1998**, *108*, 4439.

(16) Stratmann, R. E.; Scuseria, G. E.; Frisch, M. J. *J. Chem. Phys.* **1998**, *109*, 8218.

(17) Wiberg, K. B.; Oliveira, A. E. d.; Trucks, G. *J. Phys. Chem. A* **2002**, *106*, 4192.

(18) Jacquemin, D.; Preat, J.; Wathelet, V.; Fontaine, M.; Perpete, E. A. *J. Am. Chem. Soc.* **2006**, *128*, 2072.

(19) Frisch, M. J.; Trucks, G. W.; Schlegel, H. B.; Scuseria, G. E.; Robb, M. A.; Cheeseman, J. R.; Montgomery, J. A., Jr.; Vreven, T.; Kudin, K. N.; Burant, J. C.; Millam, J. M.; Iyengar, S. S.; Tomasi, J.; Barone, V.; Mennucci, B.; Cossi, M.; Scalmani, G.; Rega, N.; Petersson, G. A.; Nakatsuji, H.; Hada, M.; Ehara, M.; Toyota, K.; Fukuda, R.; Hasegawa, J.; Ishida, M.; Nakajima, T.; Honda, Y.; Kitao, O.; Nakai, H.; Klene, M.; Li, X.; Knox, J. E.; Hratchian, H. P.; Cross, J. B.; Adamo, C.; Jaramillo, J.; Gomperts, R.; Stratmann, R. E.; Yazyev, O.; Austin, A. J.; Cammi, R.; Pomelli, C.; Ochterski, J. W.; Ayala, P. Y.; Morokuma, K.; Voth, G. A.; Salvador, P.; Dannenberg, J. J.; Zakrzewski, V. G.; Dapprich, S.; Daniels, A. D.; Strain, M. C.; Farkas, O.; Malick, D. K.; Rabuck, A. D.; Raghavachari, K.; Foresman, J. B.; Ortiz, J. V.; Cui, Q.; Baboul, A. G.; Clifford, S.; Cioslowski, J.; Stefanov, B. B.; Liu, G.; Liashenko, A.; Piskorz, P.; Komaromi, I.; Martin, R. L.; Fox, D. J.; Keith, T.; Al-Laham, M. A.; Peng, C. Y.; Nanayakkara, A.; Challacombe, M.; Gill, P. M. W.; Johnson, B.; Chen, W.; Wong, M. W.; Gonzalez, C.; Pople, J. A. *Gaussian 03*, revision C.02; Gaussian, Inc.: Wallingford, CT, 2004.

(20) Becke, A. D. *Phys. Rev. A: At., Mol., Opt. Phys.* **1988**, *38*, 3098.

(21) Perdew, J. P. *Phys. Rev. B: Condens. matter Mater. Phys.* **1986**, *33*, 8822.

(22) Stephens, P. J.; Devlin, F. J.; Chabalowski, C. F.; Frisch, M. J. *J. Phys. Chem.* **1994**, *98*, 11623.

(23) Hertwig, R. H.; Koch, W. *Chem. Phys. Lett.* **1997**, *268*, 345.

(24) Hariharan, P. C.; Pople, J. A. *Chem. Phys. Lett.* **1972**, *16*, 217.

(25) Krishnan, R.; Binkley, J. S.; Seeger, R.; Pople, J. A. *J. Chem. Phys.* **1980**, *72*, 650.

(26) Frisch, M. J.; Pople, J. A.; Binkley, J. S. *J. Chem. Phys.* **1984**, *80*, 3265.

(27) Arulmozhiraja, S.; Fujii, T. *J. Chem. Phys.* **2001**, *115*, 10589.

(28) Dunlap, B. I. *J. Chem. Phys.* **1983**, *78*, 3140.

(29) Dunlap, B. I. *THEOCHEM* **2000**, *529*, 37.

(30) Clark, T.; Chandrasekhar, J.; Spitznagel, G. W.; Schleyer, P. v. R. *J. Comput. Chem.* **1983**, *4*, 294.

(31) Dobbs, K. D.; Dixon, D. A. *J. Phys. Chem.* **1996**, *100*, 3965.

(32) Lee, S. Y. *Bull. Korean Chem. Soc.* **1998**, *19*, 93.

(33) Lapouge, C.; Buntinx, G.; Poizat, O. *J. Mol. Struct.* **2003**, *651*−*653*, 747.

(34) Figures 1 and 2 display only the α orbitals of the open-shell molecules. The molecular orbitals were created with the GaussView program (see ref 35).

(35) Dennington, R., II; Keith, T.; Millam, J.; Eppinnett, K.; Hovell, W. L.; Gilliland, R. *GaussView*, revision 3.09; Semichem, Inc.: Shawnee Mission, KS, 2003.

(36) Lias, S. G. Ionization Energy Evaluation in NIST Chemistry WebBook. In *NIST Standard Reference Database Number 69*; Linstrom, P. J., Mallard, W. G., Eds.; National Institute of Standards and Technology: Gaithersburg, MD, 2005. http://webbook.nist.gov (accessed May 2006).

(37) Curtiss, L. A.; Redfern, P. C.; Raghavachari, K.; Pople, J. A. *J. Chem. Phys.* **1998**, *109*, 42.

(38) Oliveira, G. d.; Martin, J. M. L.; Proft, F. d.; Geerlings, P. *Phys. Rev. A: At., Mol., Opt. Phys.* **1999**, *60*, 1034.

(39) Rienstra-Kiracofe, J. C.; Tschumper, G. S.; Schaefer, H. F., III; Nandi, S.; Ellison, G. B. *Chem. Rev.* **2002**, *102*, 231.

(40) Vydrov, O. A.; Scuseria, G. E. *J. Chem. Phys.* **2005**, *122*, 184107.

(41) Hunter, E. P. L.; Lias, S. G. *J. Phys. Chem. Ref. Data* **1998**, *27*, 413.

(42) Davico, G. E.; Bierbaum, V. M.; DePuy, C. H.; Ellison, G. B.; Squires, R. R. *J. Am. Chem. Soc.* **1995**, *117*, 2590.

CT600242M